Temperature dependence of heat conduction in the Fermi-Pasta-Ulam-β lattice with next-nearest-neighbor coupling

Daxing Xiong,[1,*] Yong Zhang,[2,†] and Hong Zhao[2]

[1]*Department of Physics, Fuzhou University, Fuzhou 350002, Fujian, China*

[2]*Department of Physics and Institute of Theoretical Physics and Astrophysics, Xiamen University, Xiamen 361005, Fujian, China*

(Received 3 June 2013; revised manuscript received 30 September 2013; published 15 August 2014)

We show numerically that introducing the next-nearest-neighbor interactions (of appropriate strength) into the one-dimensional (1D) Fermi-Pasta-Ulam-β (FPU-β) lattice can result in an unusual, nonmonotonic temperature dependent divergence behavior in a wide temperature range, which is in clear contrast to the universal divergence manner independent of temperature as suggested previously in the conventional 1D FPU-β models with nearest-neighbor (NN) coupling only. We also discuss the underlying mechanism of this finding by analyzing the temperature variations of the properties of discrete breathers, especially that with frequencies having the intraband components. The results may provide useful information for establishing the connection between the macroscopic heat transport properties and the underlying dynamics in general 1D systems with interactions beyond NN couplings.

DOI: 10.1103/PhysRevE.90.022117 PACS number(s): 05.60.−k, 44.10.+i, 63.20.Pw, 63.20.Ry

I. INTRODUCTION

Due to the desire to predict the temperature T dependence of the thermal conductivity κ for real materials [1], i.e., $\kappa(T)$, and design (control) the solid-state thermal device [2], the study of temperature dependent heat transport properties has always been a very hot research topic [3–6]. However, for simple one-dimensional (1D) lattice systems, our understanding in this respect, both from theoretical and numerical viewpoints, is still scarce [7–9].

The theoretical study of $\kappa(T)$ in 1D lattices can trace back to the work of Peierls [10], who first bought the Boltzmann equations for phonons to provide a correct description as $\kappa \sim 1/T$ at low temperatures. Nevertheless, this conclusion only applies to the harmonic lattice with weakly nonlinear perturbations. Later Aoki *et al.* [11] applied a scaling analysis to the celebrated momentum conserving system, the 1D Fermi-Pasta-Ulam-β (FPU-β) lattice, and derived the high temperature limiting behavior $\kappa \sim T^{1/4}$. These temperature dependent behaviors at low and high temperatures have also been verified by the effective phonon theory and numerical simulations [12–14] (for the effective phonon theory applied to the momentum nonconserving systems, refer to the recent progress [15]).

However, the above studies do not take into account another key effect of κ, i.e., the size L dependence of κ. The theoretical analysis for $\kappa(T)$ usually assumed κ to be independent of L, and the numerical simulations were actually performed with a fixed and small system size. Then if κ is dependent on L, the general conclusion may be quite different.

In fact, it has now been realized by extensive studies [16–21] that for 1D momentum conserving lattices, κ generally depends on the system size and follows a power-law manner: $\kappa \sim L^{\alpha}$. The exponent α is believed to be constant and universal, although there is no general consensus on its accurate value. However, a recent study of our group [22] has reported that introducing the next-nearest-neighbor (NNN) interactions into 1D lattices can cause a breakdown of the universality. We also emphasized in that work that different microscopic dynamics may result in different macroscopic heat transport behavior.

Therefore, up to now the studies of $\kappa(T)$ and $\kappa(L)$ have been done in fact separately. So it would be desirable and interesting to combine them together to provide a whole picture of κ, i.e., to establish the function $\kappa(L,T)$. For the 1D FPU-β lattices with nearest-neighbor (NN) coupling only, Aoki *et al.* [11] have suggested such a function as $\kappa \simeq 1.2L^{\alpha}T^{-1}$ for low temperatures and $\kappa \simeq 2L^{\alpha}T^{1/4}$ for high temperatures, respectively, with α ($\alpha = 0.37 \pm 0.03$) being assumed to be universal, independent of the temperature. This result indicates that the manner of $\kappa(T)$ would not be affected by the properties of $\kappa(L)$ for the universality of α. But as pointed out by Ref. [22] that when the NNN interactions are introduced, α is shown not to be a universal constant, it is then reasonable to conjecture that the proposed formulas in Ref. [11] are no longer applicable.

In this paper we shall address the question that for general 1D lattice systems, whether or not (and if yes, how) the power-law size dependence of κ would depend on the temperature, i.e., to investigate $\alpha(T)$. With the 1D FPU-β lattices including the NNN interactions, we shall show that the divergent exponent α is no longer a constant value independent of the temperature, but instead follows a nonmonotonic temperature dependent manner. This result, together with the size dependence of κ, then provides a more complete picture of the heat conduction behavior in 1D lattice systems.

II. MODELS

The system considered is a 1D lattice including both the NN and the NNN interparticle interactions [22], whose Hamiltonian can be represented by

$$H = \sum_i \left[\frac{p_i^2}{2\mu} + V(x_{i+1} - x_i) + \gamma V(x_{i+2} - x_i) \right], \quad (1)$$

*phyxiongdx@fzu.edu.cn
†yzhang75@xmu.edu.cn

where x_i is the displacement of the ith particle from its equilibrium position and p_i its momentum. The potential takes the FPU-β type as $V(x) = \frac{1}{2}x^2 + \frac{\beta}{4}x^4$ and with $\beta = 1$ to be the main focus here. The mass μ is set to be unit. The main feature of the system is that the parameter γ $(0 \leqslant \gamma \leqslant 1)$ is tunable, which specifies the comparative strength of the NNN coupling to the NN coupling. A particular case of $\gamma = 0$ corresponds to the conventional FPU-β systems with NN coupling only. For general cases of $\gamma \neq 0$, we then give the lattices including the NNN interactions.

We note that introducing the NNN interactions can enable the systems to exhibit some particular microscopic dynamical features. For example, a crucial modification to the multibreather properties [23] and a nontrivial intrinsic phase structure [24] of solutions have recently been observed in the Klein-Gordon lattices and in the discrete nonlinear Schrödinger lattices, respectively, when the NNN interactions are considered. Such unusual microscopic dynamical details should certainly be taken into account when studying heat conduction in these systems.

We would also like to mention that including the NNN interactions can give rise to a higher order linear phonon dispersion relation. Such a particular dispersion relation has a turning point at $\gamma = 0.25$, where it has been found that [22] the discrete breathers can clearly show both intraband and extra-band components, under some nonlinearities of appropriate strengths. This nontrivial feature has also been suggested to be crucial to the nonuniversal heat conduction of this system [22]. Therefore in the following we shall give our main focus in the case of $\gamma = 0.25$ to investigate $\alpha(T)$. Such a consideration may enable us to clearly explore the role of the NNN interactions in temperature dependence of heat conduction.

III. METHODS

We employ the reverse nonequilibrium molecular dynamics (RNEMD) method to perform our simulations. This approach was first proposed for monoatomic fluids [25] and then extended to be applicable to molecular fluids [26]. The VASP [27,28] and lamps [29] codes modified to this method are also available. For the method applied to 1D lattice systems, one can refer to Ref. [22] for a detailed implementation.

To adopt the RNEMD method, one should first apply the periodic boundary conditions to the lattice, which will make the lattice form like a circle. Then the circle is divided into M ($M = 80$ used in this article) bins of equal size, each containing $n = \frac{N}{M}$ particles.

The main idea of the RNEMD method is to produce the temperature gradient by imposing the heat flux along the lattice, which can be realized by exchanging the kinetic energy (usually momentum swapping) between the predenoted cold and hot bins. In practice, we give each bin a serial number and assign the cold bin to be bin 1 and, accordingly, the hot one to be bin $M/2 + 1$. Then we artificially interchange the momentum of the hottest particle in bin 1 with that of the coldest particle in bin $M/2 + 1$ at a frequency f_{exc}. After several times interchanges, the kinetic energy of the system will redistribute with a difference. As a consequence, the relaxation of energy difference will drive two heat fluxes to flow from the hot bin to the cold bin along the two semicircular sides (with an effective length of $L = \frac{N}{2} - n$) bridging them. Then when the stationary state is eventually reached, the heat flux $\langle J \rangle$ across each side can be measured, and the temperature profile of the system will be established and can be represented by the time averaged kinetic temperature of each bin, denoted by $\langle T_k \rangle$ for bin k. The instantaneous local kinetic temperature is then calculated by $T_k \equiv \frac{1}{n\mu k_B} \sum_{i=n(k-1)+1}^{nk} p_i^2$, where k_B is the Boltzmann constant (set to be unit) and the sum runs over all n particles in bin k.

Compared with the usual method that directly brings the two ends of the lattice in contact with two heat baths at different temperatures, the RNEMD method has its advantages: It can suppress the boundary effects by imposing the periodic boundary conditions and therefore leads to a faster convergence to the stationary state. Such a comparison has been well verified in Ref. [22] where it has been shown that the RNEMD method can enable us to get a more accurate measurement of α at a relatively small L for the conventional FPU-β system with NN coupling only ($\gamma = 0$). We note that these advantages may benefit from the coarse-grained procedure, i.e., we have performed the measurement in several bins rather than per particle.

The simulation is actually performed as follows. For each temperature considered, the system is first fully thermalized to the focused temperature, then the RNEMD method is used to evolve the system by a velocity-Verlet algorithm [30] (with a time step 0.005–0.01). After a long enough time of the evolution, we then examine the temperature distribution along the system, measure the heat flux, and finally derive the heat conductivity according to the Fourier's law, during the next evolution time. The heat conductivity is obtained from $\kappa = -\langle J \rangle / \nabla T$, with the temperature gradient ∇T being evaluated over the bins between the cold and the hot one.

The difficulty of studying the heat conduction problem via the RNEMD method lies in the case of low temperatures because a lower T may need more time to ensure the system relaxed to the stationary state, which may be beyond our calculation with the existing computing resources. Therefore the lowest temperature considered is $T = 0.25$. Besides, due to the different relaxation time for the high and low temperatures, the exchange frequency f_{exc} in adopting the RNEMD method should be different, i.e., a low (high) f_{exc} is used for a low (high) temperature. For the focused temperature range $0.25 \leqslant T \leqslant 100$, f_{exc} is set from 0.0125 to 0.1 (note that in Ref. [22] $f_{\text{exc}} = 0.1$ was used) and the evolution time is about $2\times10^7 - 1\times10^9$, which has been verified to be long enough for the systems to reach the stationary state.

IV. RESULTS

Now let us see the simulation results. We show the temperature profiles first. As some examples the temperature profiles for $T = 0.25$ and $T = 30$ with the effective system size $L = 19968$ are plotted in Figs. 1(a) and 1(b), from which a well-behaved temperature profile that varies smoothly along the lattice can be clearly seen for both cases. It is worth mentioning that such a temperature profile has also been verified for other temperature values. Based on this fact, we are able to measure the heat conductivity according to

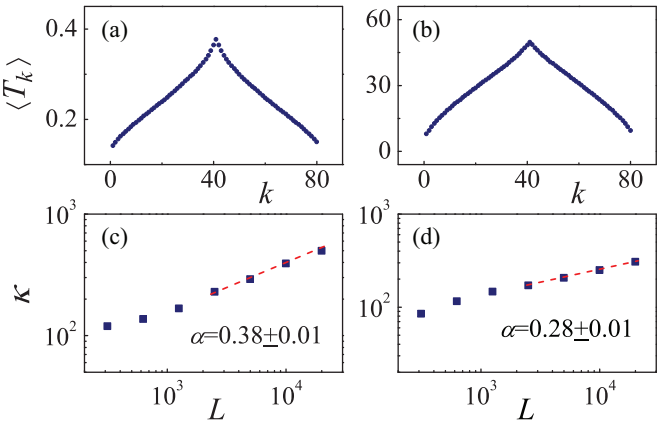

FIG. 1. (Color online) (a) and (b): The temperature profile for two typical average system temperatures $T = 0.25$ and $T = 30$, respectively. (c) and (d): The corresponding dependent properties of the heat conductivity κ on system size L; The best fitting (the dashed lines) suggest $\kappa \sim L^{\alpha}$ with $\alpha = 0.38 \pm 0.01$ and $\alpha = 0.28 \pm 0.01$, respectively.

Fourier's law. Next, in order to obtain α for each temperature from $T = 0.25$ to $T = 100$, we carefully examine the size dependence of κ. The results for the temperatures focused in Figs. 1(a) and 1(b) are plotted in Figs. 1(c) and 1(d), from which the divergence of the heat conductivity with the system size as $\kappa \sim L^{\alpha}$ can be clearly recognized; they suggest that $\alpha = 0.38 \pm 0.01$ for $T = 0.25$ and $\alpha = 0.28 \pm 0.01$ for $T = 30$, respectively. Such divergence behaviors have also been verified for other temperature values, which is in agreement with the generally accepted power-law divergent behaviors of the heat conductivity in 1D momentum conserving lattices with symmetric interparticle interactions [7,8].

We then present the results of $\alpha(T)$. The dependence of α on T is plotted in Fig. 2 (the data of the solid ones). Therein two data points are extracted from Figs. 1(c) and 1(d) while others are calculated additionally in the same way. From Fig. 2 one can see that as T increases from 0.25 to 100, a three order of T, α decreases first, reaches its minimum value at $T_{\rm tr} = 1.5$,

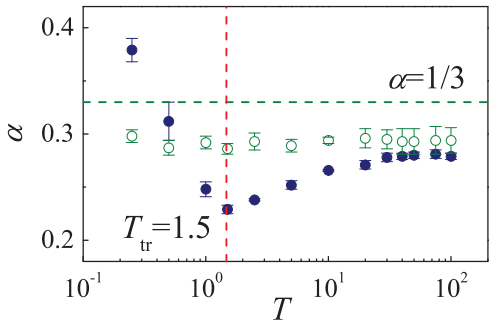

FIG. 2. (Color online) The dependence of α on the average system temperature T for FPU-β model (the solid circle) and the purely quartic FPU model (the hollow circle). Both models include the NNN couplings with a fixed ratio $\gamma = 0.25$. The error bars give the standard error for evaluating α by linearly fitting $\ln \kappa$ versus $\ln L$. The vertical dashed line indicates the turning point $T_{\rm tr} = 1.5$; the horizontal line indicates $\alpha = 1/3$ for the FPU-β model without including the NNN couplings.

then increases up to about 0.28 at $T = 100$ with a trend of saturation. Obviously, for $0.25 \leqslant T \leqslant 100$ considered here, α changes continuously and nonmonotonically with T implying that a universal α, independence of T, does not exist, which is in clear contrast to the universality of α ($\alpha = 1/3$, the most generally accepted α value, we have also denoted it in the figure for comparison), as suggested in the previous studies for the conventional FPU-β systems with NN coupling only ($\gamma = 0$) [7,8,11]. More importantly, such an unusual temperature variation of α thus suggests that the studies of $\kappa(L)$ and $\kappa(T)$ should not be taken into account separately, and the function of $\kappa(L,T)$ is more complicated when the NNN interactions are included.

The above is the main result of this paper. Interestingly, in addition to the behavior in the intermediate temperature region, the result in Fig. 2 also implies two limiting behaviors: an increased α in the low temperature range and a saturated α in the high temperature limit. For the former case, at present we have no idea that whether the α value will keep increasing towards up to $\alpha = 1$ just as the harmonic case or will decrease down to $\alpha = 0$ following the weakly anharmonic case as suggested in Ref. [31]. To answer this question, one should have to carefully investigate whether the possibility of a finite temperature phase transition [32] would take place in this system, the discussion of which is beyond the scope of the present work.

However, we can say more for the high temperature limiting case. In this limit the system is equivalent to the anharmonic limiting lattice ($\beta = \infty$). $\beta = \infty$ is not suitable for simulations. In practice one can realize it by discarding the quadratic term of the potential in the Hamiltonian [Eq. (1)], since in this case the quadratic term is negligible compared with the quartic term. Therefore the anharmonic limiting lattice is equivalent to the model having Hamiltonian with quartic term only, usually called as the purely quartic FPU model. The results of $\alpha(T)$ for the purely quartic FPU lattice with $\gamma = 0.25$ are also plotted in Fig. 2 for comparison (the data of the hollow ones). It can be seen that a value about $\alpha \simeq 0.30$, slightly larger than the saturated value ($\alpha \simeq 0.28$), clearly confirms the saturated behavior in the high temperature limit. In fact for the purely quartic FPU lattice, regardless of the interactions with or without NNN couplings, the Hamiltonian has its scaling property, i.e., $H/T = H'/T'$ under the scaling $p_i = (T/T')^{1/2} p_i'$, $x_i = (T/T')^{1/4} x_i'$ [11,33]. Such a scaling property thus leads to a universal heat conduction behavior independent of the temperature, which also supports the saturated α. We note that the mechanism of the saturated behavior may result from the scattering between solitary waves [33]. The details to support this mechanism will be presented in our further studies.

V. DISCUSSIONS

In this section we discuss the underlying mechanism of $\alpha(T)$ that was observed in the intermediate temperature region. The mechanism of heat conduction in 1D lattices is a predominant complicated problem, the solution of which should take into account many factors, such as the phonon-phonon interactions and the effects of other nonlinear excitations—the solitary waves [34] and the discrete breathers (DBs) [35]. Based on our current knowledge on this issue and

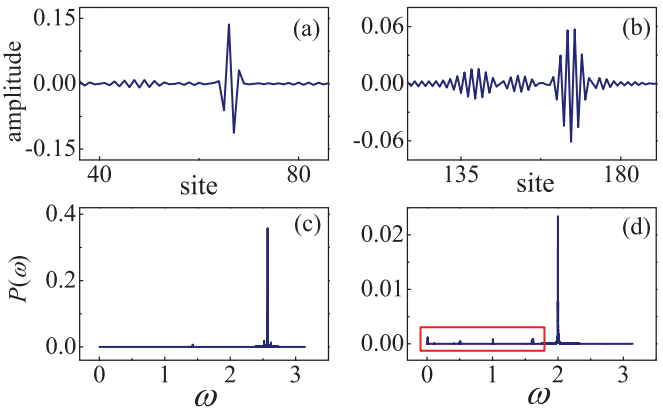

FIG. 3. (Color online) (a) and (b): Snapshots of two typical examples of DBs that randomly emerge in the lattice after a long enough time for absorption. The initial system temperature for both cases is fixed at $T = 1.5$. (c) and (d): The corresponding power spectrum $P(\omega)$ (take arbitrary units, the same hereinafter) of the DBs. The boxed region in (d) implies that kind of DBs having the intraband components.

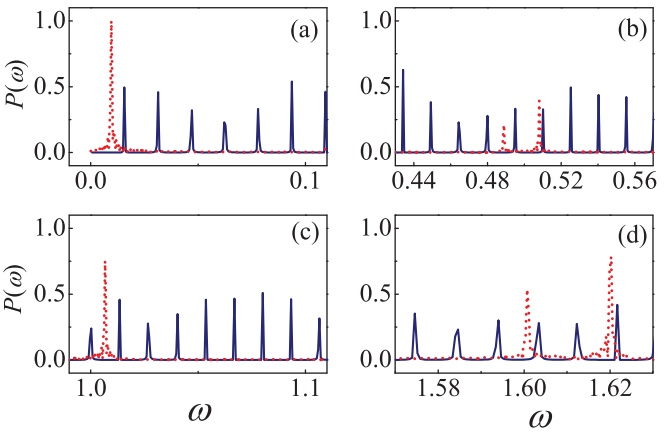

FIG. 4. (Color online) Comparison between the frequencies of the intraband components indicated in Fig. 3(d) (the dashed lines) and the phonons frequencies (the solid lines). For a better visualization, in all plots, the values of $P(\omega)$ have been rescaled between 0 and 1.

understanding of the specified model: Introducing the NNN interactions can result in unusual DBs properties at a fixed temperature [22]; in the following we shall only limit our focus on relating the mechanism to the temperature dependent DBs properties.

We first recall that DBs can be mainly classified into two categories, i.e., the extra-band ones [36,37] and the intraband ones [38–41], according to whether their frequencies are within the linear phonons band. The effects of the extra-band DBs may mainly be localizing the system energies; however, the intraband DBs can be scattering with phonons since they have frequencies lying in the phonons band. For examples, we have shown some evidences for the roles the extra-band and intraband DBs may play in heat conduction in Refs. [42] and [22], respectively.

To study T dependent DBs properties, we should identify DBs for each initial system temperature first. One can employ the following method [37,43]: A lattice of $N = 200$ particles (for facilitating the calculation) is initially thermalized to the focused temperature with Nose-Hoover heat baths [44], then the heat baths are removed and the absorbing boundary conditions are imposed. If DBs exist, after a long enough time for absorption leading all the mobile excitations, such as phonons and solitary waves absent, the DBs may show up eventually in the lattice. We have indeed seen the DBs. As some examples, two typical DBs snapshots for initial temperature $T = 1.5$ that can stably exist in the lattice are shown in Figs. 3(a) and 3(b), from which one can see that both types of DBs have a center region, suggesting that both of them can localize energies. However, the latter one looks more like an envelope soliton and has a tail away from the central region. This tail should not be the phonons since we have performed an absorption procedure for a long enough time; then if they are phonons, they should be absorbed and the tail should be absent. Further detailed examination of the frequencies of the tail has indeed confirmed that its frequencies are within the linear phonons band [see the boxed region in Fig. 3(d)], implying that the latter type of DBs contains the intraband components. We have also checked the frequencies of the DBs shown in Fig. 3(a) for comparison and confirmed that their frequencies are indeed mainly outside the phonons band [see Fig. 3(c)].

It would be interesting to make a comparison between the frequencies of these intraband components and the phonons frequencies. Figure 4 shows such a picture, from which one can see that all of the frequencies of the intraband components are penetrating inside the linear phonons spectrum [38]. This is just the popular numerical evidence that is often used to detect the DBs with intraband components (see also Refs. [39–41]).

Now that we have obtained and identified the DBs, the next step is to calculate the $P(\omega)$ for all particles along the lattice for each initial temperature, which just gives the temperature dependent DBs properties of our systems. Our main results are summarized in Fig. 5, among which (a)–(c) present the power spectrum $P(\omega)$ of the residual thermal fluctuations (can be regarded as DBs) after a long time's absorption for initial temperatures $T = 0.25$, $T = 1.5$, and $T = 30$, respectively. The time used for absorption here is

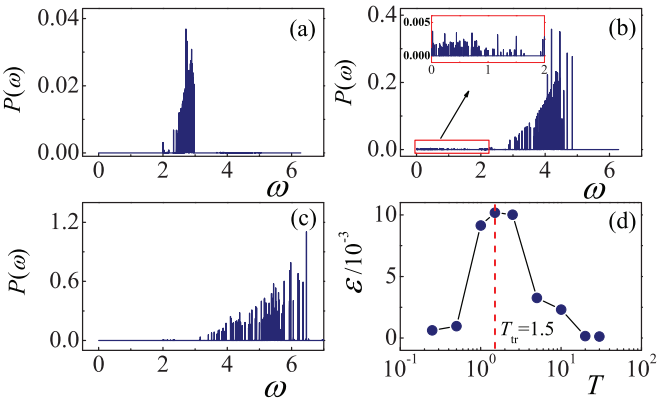

FIG. 5. (Color online) The power spectrum $P(\omega)$ of the residual thermal fluctuations for three typical initial system temperatures: (a) $T = 0.25$; (b) $T = 1.5$; (c) $T = 30$, respectively. The inset in (b) is a zoom for the boxed intraband components ($\omega \leqslant 2$). (d) The energy portion ε of the residual thermal fluctuations within the phonon band. The vertical dashed line indicates the turning point $T_{tr} = 1.5$.

about 10^6; however, we mention that we have also taken a much longer time's absorbing (about 10^7) and found the results remain unchanged, suggesting that the absorbing time used here is indeed long enough. To measure the power spectrum $P(\omega)$ for each initial temperature, we take 100 instances of simulation where different initial conditions are considered, for the average. From Figs. 5(a)–5(c) one can see a significant portion of the DBs frequencies appearing within the linear phonon band ($\omega \leqslant 2$) for initial temperature $T = 1.5$, which is in clear contrast to the cases of $T = 0.25$ and $T = 30$ [refer to the inset of Fig. 5(b) for a more clear recognition]. This result is also consistent with the analysis in Fig. 3(d).

Interestingly, Figs. 5(a)–5(c) suggest that those intraband modes are nearly absent for $T = 0.25$ and $T = 30$ but emerging most for $T = 1.5$, implying that the temperature dependent properties of the DBs with intraband components is nonmonotonic. Another piece of information is that the spectrum walk towards the direction of high frequencies with the increase of T, indicating that the energies of DBs with extra-band components ($\omega > 2$) change monotonically with T. Then our result here shows different temperature dependent properties of the intraband and the extra-band modes of DBs, i.e., the former is nonmonotonic but the latter is monotonic, which we emphasize. We will show in the following that it is crucial to the nonmonotonic properties of $\alpha(T)$ observed in our system, in contrast to the universal α as suggested previously in the conventional FPU-β system with NN coupling only, since the latter system has been shown to excite the DBs with extra-band components only [22].

A detail in Fig. 5(b) that should be mentioned is that the frequencies of these collective modes are actually discrete and emerging randomly; the reason for them looking like continuous is mainly due to the fact that we have taken 100 instances of simulation for the average here. In addition, their magnitudes are expected to be relatively small (less than 1% in the figure) because these modes may have strong interactions with phonons since their frequencies are within the phonon band. Such interactions thus lower their magnitudes. We also remind that the absorbing boundary conditions are imposed along the lattice, which may also cause the reduction of the magnitudes. However, we should emphasize that such relatively small magnitudes would not affect their effects on heat conduction in the case of thermal equilibrium when the absorptions are not imposed.

Now we have shown numerically that introducing the NNN interactions of $\gamma = 0.25$ can enable systems to excite DBs with both the extra-band and intraband components. We have also understood that the temperature dependent properties of DBs with intraband components are nonmonotonic. Then a question arises: Is there any relationship between this temperature dependence of DBs and the nonmonotonic manner of $\alpha(T)$ that we observed in Fig. 2? To answer this question, following Ref. [22], we define $\varepsilon = \int_0^2 P(\omega)d\omega / \int_0^\infty P(\omega)d\omega$, the ratio of the energy of the collective modes within the linear phonon band to the total energy of DBs, to measure the relative proportion of intraband modes and investigate how ε depends on T. To evaluate ε, for each system initial temperature focused in Fig. 2, we have calculated the corresponding power spectrum in the same way as those in Figs. 5(a)–5(c) and summarized $\varepsilon(T)$ in Fig. 5(d). From the figure one can see that as T decreases from 100 to 0.25, ε increases first, reaches its maximum value at $T_{\rm tr} = 1.5$, then decreases. Then combining the temperature dependence of α, a positive correlation between $\alpha(T)$ and $\varepsilon(T)$ can be easily recognized [see Figs. 2 and 5(d)].

Given the above positive relationship between $\alpha(T)$ and $\varepsilon(T)$, here we would like to suggest such a possible picture [45]: Suppose the scattering between phonons and the intraband modes can be described by ε, then with the change of T, this scattering will become stronger and stronger (weaker and weaker) for $0.25 \leqslant T \leqslant T_{\rm tr}$ ($T_{\rm tr} \leqslant T \leqslant 100$). As a stronger (weaker) scattering will finally limit (facilitate) the heat transport in the thermodynamic limit, our results in Figs. 2 and 5(d) are in very good accord with this picture.

VI. CONCLUSIONS

To summarize, we have numerically studied the temperature dependence of heat conduction behavior of the 1D FPU-β lattice when the NNN interactions are considered. For a fixed coupling ratio $\gamma = 0.25$, we have found that in the wide temperature range ($0.25 \leqslant T \leqslant 100$) considered, although a power-law divergence of the heat conductivity with the system size, i.e., $\kappa \sim L^\alpha$, can still be seen, and the value of α does not show universality any more: It nonmonotonically changes with the temperature. This result is in contrast to the existence of a fixed α independent of the temperature as suggested in the conventional FPU-β lattice with NN coupling only. Such an unusual result, together with the size dependence of the heat conductivity, then provides a more complete picture of the heat conduction behavior.

In order to well understand this temperature variation of heat conduction, we have also numerically investigated how the properties of DBs depend on the temperature. The temperature dependent properties of DBs with the intraband components is shown to be nonmonotonic with a turning point at $T_{\rm tr} = 1.5$, in contrast to that of the extra-band modes. Such a nonmonotonic manner shows a positive correlation with the temperature dependent properties of α, which is consistent with the assumption that DBs, especially those with intraband components, can provide a phonon scattering mechanism contributing to heat conduction. This finding is suggestive for our understanding of heat conduction from the microscopic dynamic viewpoints, although a detailed mechanism of phonon-DBs interactions has not been given here. Finally, one open question left is why for both α and the intraband modes there exists such a turning temperature point of $T_{\rm tr} = 1.5$, which we are interested in and wish to understand via further studies.

ACKNOWLEDGMENTS

We thank J. Wang for useful discussions and kind help in preparing the manuscript. This work was supported by the NNSF (Grants No. 11205032, No. 11335006, and No. 11147191) of China, the NSF (Grant No. 2013J05008) of Fujian province and the startup fund (No. 022390) of Fuzhou University.

[1] J. P. Francoise, G. L. Naber, and T. S. Tsun, *Encyclopedia of Mathematical Physics: Equilibrium Statistical Mechanics; Nonequilibrium Statistical Mechanics* (Science Press, Beijing, China, 2008).

[2] C. W. Chang, D. Okawa, A. Majumdar, and A. Zettl, Science **314**, 1121 (2006).

[3] J. Hone, M. Whitney, C. Piskoti, and A. Zettl, Phys. Rev. B **59**, R2514 (1999).

[4] P. Kim, L. Shi, A. Majumdar, and P. L. McEuen, Phys. Rev. Lett. **87**, 215502 (2001).

[5] C. W. Chang, A. M. Fennimore, A. Afanasiev, D. Okawa, T. Ikuno, H. Garcia, Deyu Li, A. Majumdar, and A. Zettl, Phys. Rev. Lett. **97**, 085901 (2006).

[6] E. Pop, D. Mann, Q. Wang, K. Goodson, and H. Dai, Nano Lett. **6**, 96 (2006).

[7] S. Lepri, R. Livi, and A. Politi, Phys. Rep. **377**, 1 (2003).

[8] A. Dhar, Adv. Phys. **57**, 457 (2008).

[9] J. Lebowitz, S. Olla, and G. Stoltz, Final report of workshop Nonequilibrium statistical mechanics: mathematical understanding and numerical simulation.

[10] R. Peierls, Ann. Phys. (Leipzig) **395**, 1055 (1929).

[11] K. Aoki and D. Kusnezov, Phys. Rev. Lett. **86**, 4029 (2001).

[12] N. Li and B. Li, Europhys. Lett. **75**, 49 (2006); **78**, 34001 (2007); Phys Rev. E **76**, 011108 (2007).

[13] D. He, S. Buyukdagli, and B. Hu, Phys. Rev. E **78**, 061103 (2008).

[14] N. Li and B. Li, AIP Adv. **2**, 041408 (2012).

[15] N. Li and B. Li, Phys Rev. E **87**, 042125 (2013).

[16] G. Casati, J. Ford, F. Vivaldi, and W. M. Visscher, Phys. Rev. Lett. **52**, 1861 (1984); S. Lepri, R. Livi, and A. Politi, *ibid.* **78**, 1896 (1997); T. Prosen and D. K. Campbell, *ibid.* **84**, 2857 (2000); B. Li, G. Casati, J. Wang, and T. Prosen, *ibid.* **92**, 254301 (2004); T. Prosen and D. K. Campbell, Chaos **15**, 015117 (2005).

[17] O. Narayan and S. Ramaswamy, Phys. Rev. Lett. **89**, 200601 (2002); T. Mai and O. Narayan, Phys. Rev. E **73**, 061202 (2006); T. Mai, A. Dhar, and O. Narayan, Phys. Rev. Lett. **98**, 184301 (2007); H. Van Beijeren, *ibid.* **108**, 180601 (2012).

[18] G. R. Lee-Dadswell, B. G. Nickel, and C. G. Gray, Phys. Rev. E **72**, 031202 (2005); J. Stat. Phys. **132**, 1 (2008); L. Delfini, S. Lepri, R. Livi, and A. Politi, Phys. Rev. E **73**, 060201(R) (2006); J. Stat. Mech. (2007) P02007; J.-S. Wang and B. Li, Phys. Rev. Lett. **92**, 074302 (2004); Phys. Rev. E **70**, 021204 (2004).

[19] B. Hu, B. Li, and H. Zhao, Phys. Rev. E **57**, 2992 (1998); **61**, 3828 (2000).

[20] Y. Zhong, Y. Zhang, J. Wang, and H. Zhao, Phys. Rev. E **85**, 060102(R) (2012); S. Chen, Y. Zhang, J. Wang, and H. Zhao, arXiv:1204.5933v3; L. Wang, B. Hu, and B. Li, Phys. Rev. E **88**, 052112 (2013); A. V. Savin and Y. A. Kosevich, *ibid.* **89**, 032102 (2014).

[21] C. W. Chang, D. Okawa, H. Garcia, A. Majumdar, and A. Zettl, Phys. Rev. Lett. **101**, 075903 (2008).

[22] D. Xiong, J. Wang, Y. Zhang, and H. Zhao, Phys. Rev. E **85**, 020102(R) (2012).

[23] V. Koukouloyannis, P. G. Kevrekidis, J. Cuevas, and V. Rothos, Physica D **242**, 16 (2013); Z. Rapti, Phys. Lett. A **377**, 1543 (2013).

[24] P. G. Kevrekidis, Phys. Lett. A **373**, 3688 (2009); C. Chonga, R. Carretero-Gonzlez, B. A. Malomed and P. G. Kevrekidis, Physica D **240**, 1205 (2011).

[25] F. Müller-Plathe, J. Chem. Phys. **106**, 6082 (1997).

[26] D. Bedrov and G. D. Smith, J. Chem. Phys. **113**, 8080 (2000).

[27] S. Stackhouse, L. Stixrude, and B. B. Karki, Phys. Rev. Lett. **104**, 208501 (2010).

[28] D. Wang, L. Tang, M. Long, and Z. Shuai, J. Phys. Chem. C **115**, 5940 (2011).

[29] http://lammps.sandia.gov.

[30] M. P. Aüllen and D. L. Tildesley, *Computer Simulation of Liquids* (Clarendon, Oxford, 1987).

[31] K. Aoki, J. Lukkarinen, and H. Spohn, J. Stat. Phys. **124**, 1105 (2006).

[32] S. G. Das, A. Dhar, and O. Narayan, J. Stat. Phys. **154**, 204 (2014).

[33] H. Zhao, Phys. Rev. Lett. **96**, 140602 (2006); H. Zhao, Z. Wen, Y. Zhang, and D. Zheng, *ibid.* **94**, 025507 (2005).

[34] Y. V. Kartashov, B. A. Malomed, and L. Torner, Rev. Mod. Phys. **83**, 247 (2011).

[35] S. Flach and C. R. Willis, Phys. Rep. **295**, 181 (1998); S. Aubry, Physica D **216**, 1 (2006); S. Flach and A. V. Gorbach, Phys. Rep. **467**, 1 (2008).

[36] O. V. Gendelman and A. V. Savin, Phys. Rev. Lett. **84**, 2381 (2000); C. Giardinà, R. Livi, A. Politi, and M. Vassalli, *ibid.* **84**, 2144 (2000).

[37] G. P. Tsironis, A. R. Bishop, A. V. Savin, and A. V. Zolotaryuk, Phys. Rev. E **60**, 6610 (1999).

[38] G. Kopidakis and S. Aubry, Physica D **130**, 155 (1999); **139**, 247 (2000); Phys. Rev. Lett. **84**, 3236 (2000); S. Aubry and R. Schilling, Physica D **238**, 2045 (2009).

[39] D. Bonart, T. Rossler, and J. B. Page, Physica D **113**, 123 (1998).

[40] D. Bonart, Phys. Lett. A **233**, 233 (1997).

[41] R. Lai, S. A. Kiselev, and A. J. Sievers, Phys. Rev. B **56**, 5345 (1997).

[42] D. Xiong, Y. Zhang, and H. Zhao, Phys. Rev. E **88**, 052128 (2013).

[43] G. P. Tsironis and S. Aubry, Phys. Rev. Lett. **77**, 5225 (1996).

[44] S. Nose, J. Chem. Phys. **81**, 511 (1984); W. G. Hoover, Phys. Rev. A **31**, 1695 (1985).

[45] T. Cretegny, S. Aubry, and S. Flach, Physica D **119**, 73 (1998); M. Johansson and S. Aubry, Phys. Rev. E **61**, 5864 (2000); K. Ø. Rasmussen, S. Aubry, A. R. Bishop, and G. P. Tsironis, Eur. Phys. J. B **15**, 169 (2000); S. Flach, A. E. Miroshnichenko, and M. V. Fistul, Chaos **13**, 596 (2003).